

A low-temperature synthesis of ultraviolet-light-emitting ZnO nanotubes and tubular whiskers

Jinping Liu, Xintang Huang*

Center of Nano-Science and Technology, Department of Physics, Central China Normal University, 152-7 Luo Yu Road, Wuhan 430079, China

Received 24 October 2005; received in revised form 5 December 2005; accepted 6 December 2005

Available online 20 January 2006

Abstract

We have successfully synthesized single-crystal ZnO nanotubes and tubular whiskers by employing $\text{Zn}(\text{NO}_3)_2 \cdot 6\text{H}_2\text{O}$, $\text{NH}_3 \cdot \text{H}_2\text{O}$ as the starting materials in the presence of polyethylene glycol (PEG, $M_w = 2000$) at ambient pressure and low temperature (70°C). Characterizations are carried out by X-ray powder diffraction (XRD), X-ray energy dispersive spectroscopy (EDS), scanning electron microscopy (SEM), transmission electron microscopy (TEM, HRTEM) and photoluminescence (PL) measurement. The results show that the as-prepared ZnO are tubular textures, which have average cross-sectional dimensions of 200–300 nm, lengths of 2–3.5 μm , and wall thickness of 80 nm. These tubular products demonstrate a sharp ultraviolet excitonic emission peak centered at 385 nm at room temperature. A possible growth mechanism and the influence of the reaction temperature on the formation of crystalline ZnO are presented.

© 2005 Elsevier Inc. All rights reserved.

Keywords: Crystal morphology; Photoluminescence; Growth from solutions

1. Introduction

Since the first discovery of carbon nanotubes in 1991 [1], considerable attention has been paid to study on one-dimensional (1D) nanostructured materials [2–4] including nanorods, nanowires and nanotubes, because of their remarkable physical properties and potential applications. Among these 1D structures, tubular or hollow texture is highly desired for new technological applications [5–7], due to its superior optical, electrical, thermal and mechanical properties; its high porosity and large surface area that fulfills the demand of high efficiency and activity. Accordingly, over the past few years, inorganic nano/micro-tubes of WS_2 [8], MoS_2 [9], TiO_2 [10], V_2O_5 [11] have been successfully fabricated.

The wurtzite ZnO is a direct wide band gap (3.37 eV) semiconductor with a large excitonic binding energy (60 meV). Due to its particular physical properties, ZnO has attracted much interest for its fundamental research

and potential device applications including electrical, optoelectronic, photovoltaic devices, and sensors [12]. The morphologically controllable synthesis of ZnO nanomaterials with special size and structure is one of the key issues in material science and consciously accelerated by the success in the realization of room-temperature UV lasing from ZnO film [13]. To date, the synthesis of ZnO 1D, 2D and 3D structures such as nanowires [13], nanorods [14], nanosheets [15], nanobelts [16], nanorings, nanosprings, nanosaws, nanopropellers, disks, nanojunction arrays and dendritic patterns [12a,12b,17] have been widely demonstrated. To our knowledge, relatively few researches on the preparation of 1D ZnO structures with tubular or hollow texture have been reported [7,18–23]. In these reports, however, the obtained tubular structured ZnO is constructed not from a single crystal but many polycrystals [18]. Moreover, high temperature (400–1300 $^\circ\text{C}$) [19–22] and complex process (catalyst [22] and long reaction time [7a]) are necessary to obtain single-crystal ZnO nano- or micro-tubes. Therefore, exploring a simple route to prepare ZnO nanotubes or tubular whiskers, for answering the demand of the development of novel devices and industrial

*Corresponding author. Fax: +86 276 786 1185.

E-mail address: xthuang@phy.ccnu.edu.cn (X. Huang).

needs of low-cost large-scale production techniques, is urgent and still remains a challenge.

Wet chemical method is one of the most popular and widespread techniques in nanomaterial preparation, because of its easy and low-cost procedure, greater control over experimental parameters and convenience for synthesis in high quantities. Vayssieres et al. [7a] reported the synthesis of ZnO tubes in aqueous solution at 90 °C for 2 days by aging. However, the diameter of the tubes was too large (1–2 μm). Li et al. [23] demonstrated a solution method (heating with a reflux condenser) to prepare ZnO nanotubes at 95 °C. But the obtained tubes grew on the top faces of ZnO nanorods as secondary product with relatively poor single-crystal nature. In addition, ZnO tubes must grow from ZnO rods in the above two papers, and the preparation of ZnO rods typically involved substrates with or without ZnO seed layer. There was no report on the synthesis of ZnO nanotubes by a “one-step” magnetic stirring route with further reducing the growth temperature until now. Moreover, an explanation about the growth mechanism, as well as the realization of high optical quality of ZnO nanotubes is still desired to improve the synthesis process and technical application. In this Letter, a rational synthesis of single-crystal ZnO nanotubes and tubular whiskers by a facile process (low-cost materials, simple experimental devices, ambient pressure, 70 °C) is successfully presented. The specific formation mechanism and the strong photoluminescence (PL) at ~385 nm of the nanostructure are also discussed.

2. Experimental section

All the chemicals used in our experiments are analytical grade reagents without further purification. The detailed experimental process is described as follows. Firstly, an aqueous solution of Zn(NO₃)₂ (0.027 M) was prepared at room temperature in a glass bottle without seal under magnetic stirring by adding Zn(NO₃)₂·6H₂O (2.0 g) into 250 ml distilled water. Then, polyethylene glycol (PEG) (0.15 g, *M_w* = 2000) and 1 mol/L NH₃·H₂O were dispersed in the above-prepared Zn(NO₃)₂ solution. Finally, the obtained mixture (pH = 10) was heated to 70 °C and continued with this constant temperature until the reaction was complete (24 h). Vigorous stirring was maintained throughout the entire process. After the reaction, it was noticed that only about 50 ml solution left because of the evaporation of water. The precipitation was filtered out, washed several times with alcohol and water, and then dried at 60 °C under air atmosphere. In order to investigate the growth mechanism and the action of temperature, the experiments were also carried out at 60 and 80 °C, respectively.

The phase purity of the as-prepared products was characterized by X-ray powder diffraction (XRD) using a Y-2000 X-ray diffractometer with CuKα radiation (λ = 0.15418 nm). Scanning electron microscopy (SEM) images were obtained on a JSM-6700F microscope.

Transmission electron microscopy (TEM, HRTEM) observations were carried out on a JEOL JEM-2010 operated at 200 kV in bright field and selected-area electron diffraction modes. Room-temperature PL spectra were recorded on a JY-Labram spectrometer with a continuous-wave He–Cd laser focused at about 2 μm as the exciting source at 325 nm.

3. Results and discussion

The XRD pattern of the as-grown ZnO sample is shown in Fig. 1(a). All the diffraction peaks could be indexed to hexagonal wurtzite structure of ZnO with cell constants of *a* = 0.324982 and *c* = 0.520661 nm. No diffraction peaks from impurities are detected. In addition, the (002) reflection plane is extremely weak compared with the standard reflection, which is due to the fact that the (00*n*) planes are absent in hollow or tubular ZnO structure [7a]. Energy dispersive spectroscopy (EDS) result shown in Fig. 1(b) indicates that the as-grown sample is only composed

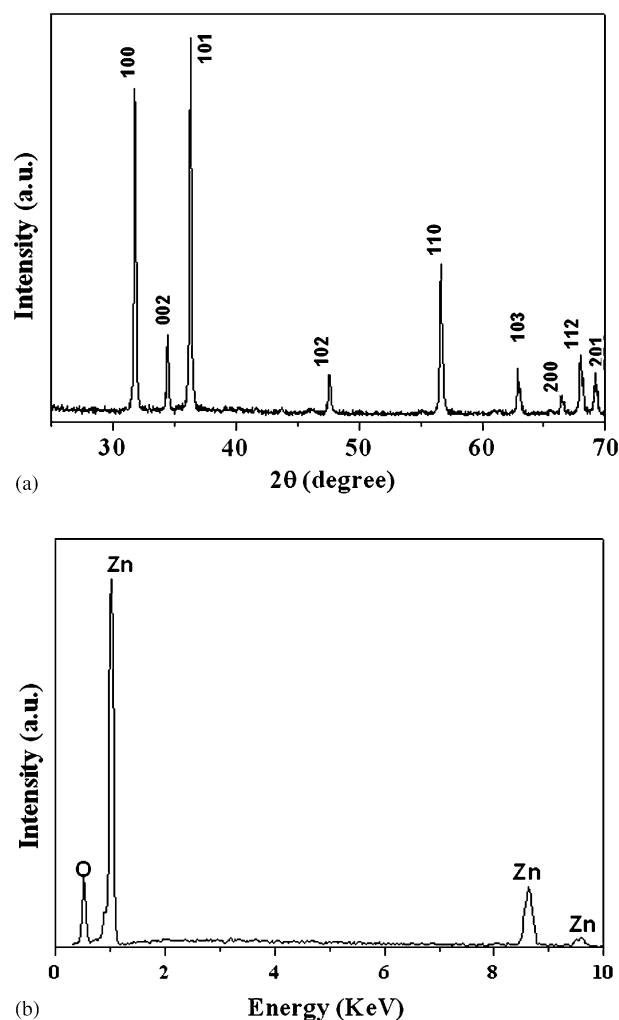


Fig. 1. (a) XRD pattern of the as-prepared ZnO tubular structures revealing the wurtzite phase and (b) EDS spectrum taken from the ZnO tubular structures.

of Zn and O, and the atomic ratio of Zn and O is about 50.43:49.57.

The general morphology of the as-prepared ZnO product is demonstrated in Fig. 2. As can be seen from a panoramic SEM image (Fig. 2(a)), the sample is composed of a large quantity of straight rods and a small amount of irregular ones. Most of the rods have fairly uniform diameters of about 250 nm (smaller than that in Ref. [18]) and lengths of up to 2 μm . More interesting, a careful examination of Fig. 2(a) suggests that most rods display hollow structures, which are specially marked using white arrows. The wall thickness of ZnO hollow rods falls in the range of 60–120 nm. Based on the above observation, we name the product “ZnO nanotubes”. Fig. 2(b) and (c) show two typical morphologies of the ZnO nanotubes with different wall thickness. It can be seen clearly that this kind (Type A) of products display uniform diameters along the growth direction. In addition, an open-ended structure of well-defined crystallographic facets and prismatic hexagon can be observed. As shown in Fig. 2(c), the hollow cavity of ZnO nanotubes also has regular prismatic hexagon. This character combined with 1D morphology suggests the large anisotropic growth characteristics of a typical ZnO crystal [7a,26], and the growth direction is along [0001] (*c*-axis).

Fig. 3(a) shows another kind (Type B: tubular whiskers) of ZnO structures observed in the product, which tend to form cluster-like morphology. It can be clearly observed that most of these whiskers exhibit non-uniform diameters

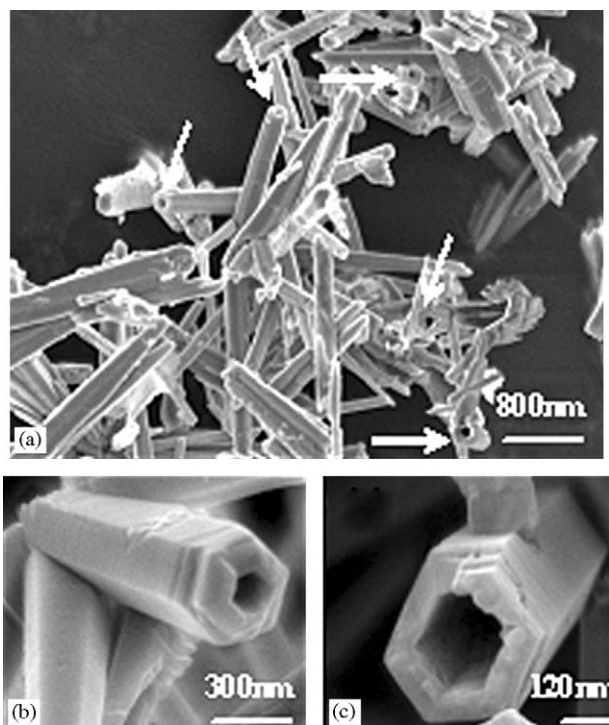


Fig. 2. (a) Panoramic SEM image of the as-prepared ZnO nanotubes. The marked white arrows indicate the open ends. (b,c) Enlarged SEM images of ZnO nanotubes with different wall thickness. Both the images shown in (b) and (c) demonstrate a typical open-ended structure of well-defined crystallographic facets and prismatic hexagon.

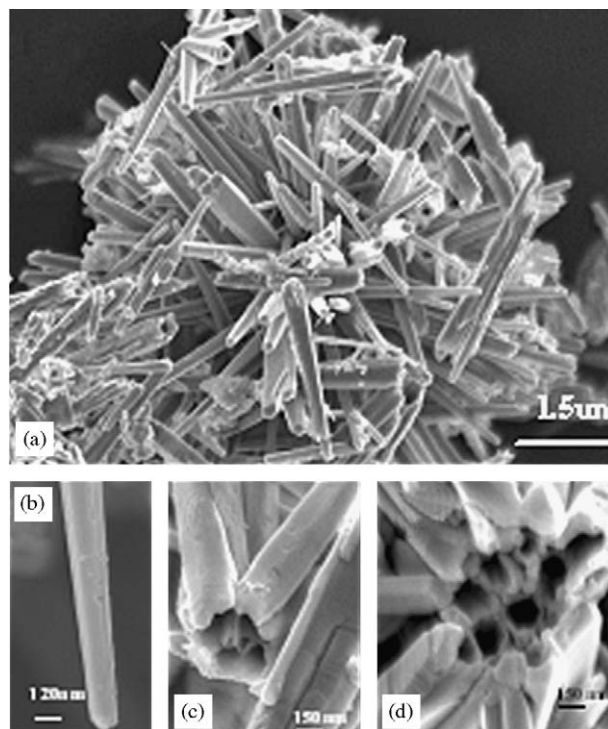


Fig. 3. (a) Panoramic SEM image of the ZnO tubular whisker clusters in the product. (b) Enlarged SEM image of an individual ZnO rod-like whisker with a closed-end tip and non-uniform diameter along the *c*-axis. (c,d) SEM images on the bottom of several attached ZnO whiskers showing the hollow and tubular structure.

along the growth direction, with smaller tips and larger bottoms (Fig. 3(a), (b)). While the average diameter of these whiskers is ~ 250 nm, the average length of them is apparently more than 2.5 μm , which is different from that in Fig. 2. In addition, the tips are closed, as shown in Fig. 3(b). Further characterizations, displayed in Fig. 3(c) and (d), show that the larger bottoms which usually attach to each other, exhibit completely open structure. That means, these ZnO whiskers are in the form of open bottoms and closed tips. In fact, they are formed with distinctive mechanism and will be discussed below.

Fig. 4(a) shows a typical TEM image of an individual ZnO whisker with a smaller tip and a larger bottom (Type B). The contrast (the outer part is darker than the inner part along the length) suggests a hollow internal core. Moreover, the dimension of this hollow internal core decreases gradually along the length and gives a closed-end tip, which is in good agreement with the SEM observations. Because the diameter of ZnO whisker is relatively large, the contrast, assuming the form of tubular whisker, is not obvious [21]. Further investigation has been carried out by SAED (inset of Fig. 4(a)) and HRTEM (Fig. 4(b)). The SAED patterns taken from different parts of the whisker show exactly the same single-crystal nature and can be indexed as [100] zone axis of hexagonal ZnO. Many other whiskers have been examined using this method, and the diffraction patterns demonstrate that all of them grow

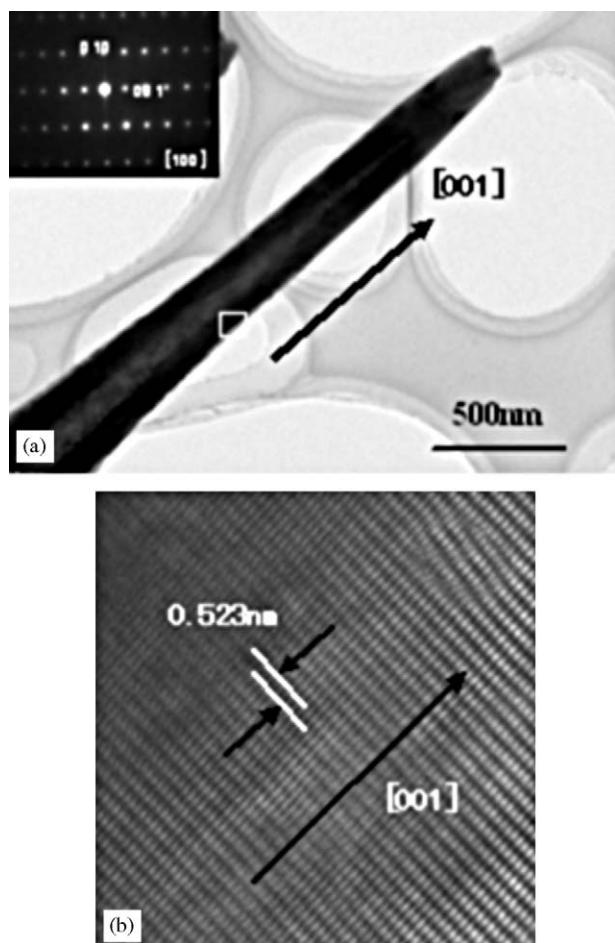


Fig. 4. (a) TEM image of an individual ZnO tubular whisker. Inset showing its corresponding SAED pattern. (b) HRTEM image of the whisker.

along the c -axis. HRTEM result, recorded from the area labeled by a rectangle in Fig. 4(a), further confirms the single-crystal characteristic and c -axis orientation of ZnO crystals.

The room-temperature PL spectra of the ZnO nanotubes and tubular whiskers were shown in Fig. 5. The 325 nm laser was focused at $\sim 2 \mu\text{m}$ and the excitation power was controlled by a neutral density filter. All the curves obtained under different excitation powers show strong UV emission at $\sim 385 \text{ nm}$ (3.23 eV), agreeing the near band edge emission [12b,18,24]. With increase of excitation power from 0.04 mW (10^{-3} W) to 0.25 mW, the sharp UV peak increases linearly (see inset of Fig. 5) without apparent shift and the FWHM is also unchanged, indicating the strong and sharp UV emission originates from the recombination of free or bound excitons [12b]. Generally, a green-yellow emission could be observed in the PL spectrum, which comes from the recombination of photo-generated hole with a singly ionized charge state of specific defect [15,20,21]. However, this kind of emission in our sample can be negligible compared with the very intensive sharp UV emission. When the excitation power is 0.25 mW, the intensity ratio of the UV to the green-yellow

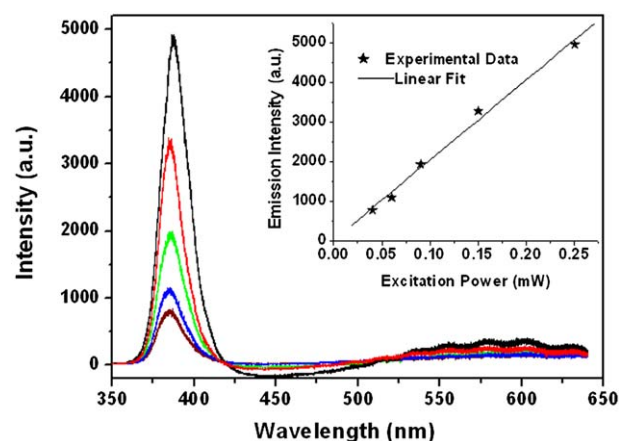


Fig. 5. Room-temperature PL spectra of the as-prepared ZnO nanotubes and tubular whiskers excited with different powers. The curves from bottom to top correspond to the excitation power of 0.04, 0.06, 0.09, 0.15 and 0.25 mW, respectively. The inset is PL intensity versus excitation power.

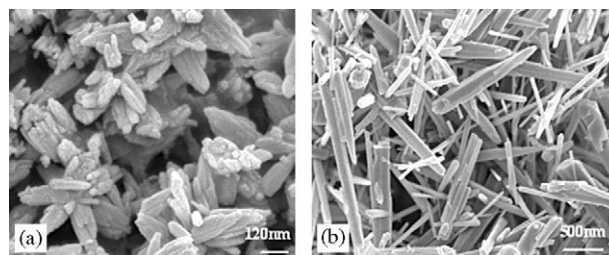


Fig. 6. ZnO nanocrystals prepared at the reaction temperature of 60 °C (a) and 80 °C (b), respectively.

emission is ~ 13 , which is nothing less than that recorded from the high-quality ZnO samples prepared by other research groups using high-temperature CVD or MBE methods [12c,12d]. Therefore, the results of PL spectra show that our low-temperature (70 °C) growth method can produce a low concentration of oxygen defects and high optical quality of single-crystal ZnO nanotubes. It is well known that drastic growth conditions such as high temperature and high pressure, or oxygen-deficient environment usually induce more defects in crystals [12b,17b]. Comparatively, as discussed above, the quality of our sample is much improved by a mild solution process. We attribute the good optical quality to the sufficient oxygen supply from ambience and mild ion transportation in solution.

In our experiment, we find that reaction temperature is a key factor for obtaining ZnO nanotubes and tubular whiskers. Fig. 6(a) and (b) shows the SEM images of ZnO crystals prepared at 60 and 80 °C, respectively. Fig. 6(a) shows that the products prepared at the temperature of 60 °C usually are bundled nanorods with average diameter of 50 nm. Comparatively, the ZnO crystals prepared at 80 °C are whisker-like and have a wide diameter

distribution of 50–250 nm. No tubular structures are observed under these two conditions.

As we know, in the absence of surfactant, ZnO usually crystallizes through a growth-directed process [25]. In this case, the formation of ZnO crystals is determined by the intrinsic crystallographic structure. However, in the presence of surfactant, the growth process is also affected by the structure-directing and control action of surfactant [14,25]. In our synthetic route, as to the growth direction of ZnO nanotubes and tubular whiskers (along [0001]), the polar crystal habit should be taken into consideration. The typical crystal habit exhibits a positive polar plane which is rich in Zn and a negative polar plane which is rich in O. In addition, the growth velocities in different directions are reported to be $V_{[0001]} > V_{[-101-1]} > V_{[-1010]} > V_{[-1011]} > V_{[000-1]}$ when a hydrothermal route is employed [26]. Accordingly, the most stable crystal structure is a regular prismatic hexagon elongated along the *c*-axis (Fig. 2(c)). Under the strong basic solution of pH = 10, the quantity of $\text{Zn}(\text{NH}_3)_4^{2+}$ is larger, and there is enough free Zn^{2+} decomposed from $\text{Zn}(\text{NH}_3)_4^{2+}$ for the formation of growth unit ($\text{Zn}(\text{OH})_4^{2-}$) [18,26]; therefore, the growth along *c*-axis is successfully favored.

As to the formation of tubular-like structure, the external conditions of surfactant PEG (2000) and growth temperature play important roles. Although the formation mechanism of ZnO nanotubes and tubular whiskers is not very clear, we can state that it is completely different from the “gas–liquid equilibrium” mechanism discussed by Zhang et al. [18], because NH_3 can escape to some extent in our experimental process. In addition, it is reasonable to give a phenomenological explanation based on all of our experimental results. Fig. 7 shows the schematic growth diagram of ZnO crystals prepared under different temperatures.

In previous works [27a,28], PEG was found favorable for obtaining 1D nanoscale materials due to its soft-template function. We also demonstrated that PEG could influence the anisotropic growth and the morphology of nanocrystals [27b]. In this study, the role of PEG in the formation of ZnO tubular structures seems to be like that

in the growth of polyoxometalates micro-tubes as described by Kang et al. [28]. The only difference is that in our case the effect of temperature must be considered. The chain-like structures of non-ionized surfactant PEG in water could form many 1D liquid reaction fields and therefore strictly limit the growth process in such divided linear spaces [28], as shown in Fig. 7. As mentioned by Kang et al. [28], the larger the concentration of water, the broader the 1D reaction field becomes. In the initial stage, at the temperature of 70 °C, the ZnO nucleated and grew into crystal in a broad linear reaction field, leading to a large dimension of diameter. Furthermore, the sufficiently broad reaction field can embrace the PEG aggregate and induce the tubular-like structure [28]. We believed that each curved PEG molecule served as a small reactor (we considered it as soft template) in that case. As we know, the atom O in the chain of C–O–C in PEG has strong coordination abilities with metal ions [27]. Therefore, in the embrace and curliness process of PEG molecule, there were many Zn^{2+} adsorbed tightly on both sides of the long chain (see Fig. 7) due to the outside ion transportation, which could make the reaction and crystallization occur in the specific spots rather than the central part of the curved reactor, resulting in the formation of hollow or tubular structures. As the reaction time increased, some growth process finished and ZnO nanotubes with uniform diameter along the *c*-axis could be formed (Fig. 2) because of slight change of the concentration of water. It is noteworthy to stress that the “embrace” should take place on many adjacent PEG molecules in all three dimensions simultaneously. With further increasing the time, some other under-developed ZnO experienced the growth development in a limited 1D reaction field (without “embrace” action [28]) due to the decrease of water. Undoubtedly, this continuous suppress of the 1D linear reaction field, resulting from the continuous decrease of the water, gave another kind of tubular-like ZnO with large open bottoms and small closed tips (Fig. 3). When at the temperature of 60 °C, it was believed that the embrace of PEG aggregate was not effective for obtaining tubular structure, and the

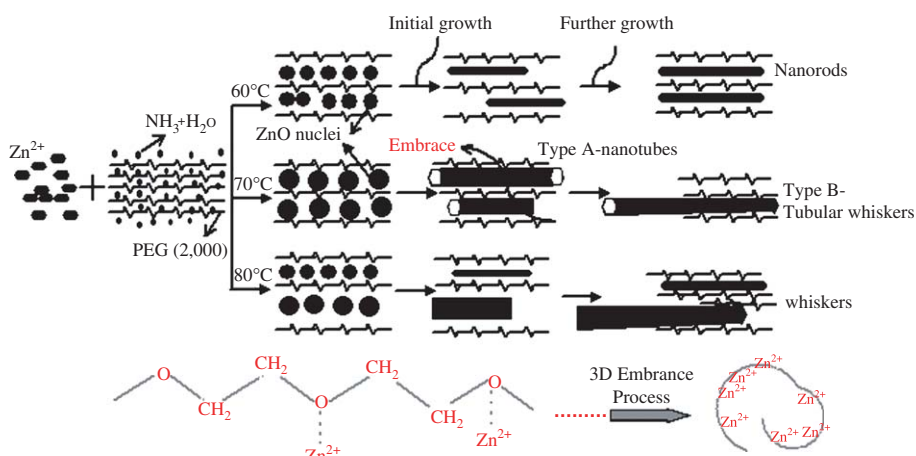


Fig. 7. Growth schematic diagrams of the ZnO crystals prepared at different temperatures in the presence of PEG.

decrease of water can be ignored. Therefore, ZnO nanorods, with relatively uniform diameter along the length, formed naturally. Furthermore, the ZnO seed crystals obtained at lower temperature tended not to aggregate into larger ones, which led to smaller diameter of the final product. With increasing temperature to 80 °C, both the embrace of PEG aggregate and the uniformity of the 1D reaction field were completely destroyed (Fig. 7). Under this condition, only ZnO whiskers having large-diameter distribution can be obtained. During the reaction period, several tubes (Fig. 3(c), (d)) or rods (Fig. 6(a)) could fuse together [28], which might result from intertwist between the PEG molecules. Further research on the complete elucidation of growth mechanism and the realization of better morphology is still under progress. Understanding of the tubular structures will be helpful for various applications.

4. Conclusion

In summary, this present work demonstrates the rational synthesis of ZnO nanotubes and tubular whiskers at a low temperature (70 °C) by a wet chemical route. The products are single-crystal in nature and exhibit strong UV excitonic emission at ~385 nm with a negligible defect emission, indicative of their high crystal quality. Comparative investigation indicates that PEG and the reaction temperature play important roles in the formation process. These novel tubular structures may well be used in nano-optoelectronics (UV light source), catalysis and waveguides [18], etc.

Acknowledgments

The authors appreciate the financial support of National Science Foundation of China (No. 50202007). We also thank the Center of Physics and Chemistry at University of Science and Technology of China for the PL measurement.

References

- [1] S. Iijima, *Nature (London)* 354 (1991) 56.
- [2] V.F. Puentes, K.M. Krishnan, A.P. Alivisatos, *Science* 291 (2001) 2115.
- [3] J.D. Holmes, K.P. Johnston, R.C. Doty, B.A. Korgel, *Science* 287 (2000) 1471.
- [4] J.T. Hu, T.W. Odom, C.M. Lieber, *Acc. Chem. Res.* 32 (1999) 435.
- [5] F. Caruso, R.A. Caruso, H. Mohwald, *Science* 282 (1998) 1111.
- [6] Y. Sun, Y. Xia, *Science* 298 (2002) 2176.
- [7] (a) L. Vayssieres, K. Keis, A. Hagfeldt, S.E. Lindquist, *Chem. Mater.* 13 (2001) 4395;
(b) H.D. Yu, Z.P. Zhang, M.Y. Han, X.T. Hao, F.R. Zhu, *J. Am. Chem. Soc.* 127 (2005) 2378.
- [8] A. Rothschild, R. Popovitz-biro, O. Lourie, R. Tenne, *J. Phys. Chem. B* 104 (2000) 8976.
- [9] Y. Feldman, E. Wasserman, D.J. Srolovitz, R. Tenne, *Science* 267 (1995) 222.
- [10] T. Kasuga, M. Hiramatsu, A. Hoson, T. Sekino, K. Niihara, *Langmuir* 14 (1998) 3160.
- [11] B.C. Satishkumar, A. Govindaraj, E.M. Vogl, L. Basumallick, C.N.R. Rao, *J. Mater. Res.* 12 (1997) 604.
- [12] (a) Z.L. Wang, *J. Phys.: Condens. Matter* 16 (2004) R829;
(b) B.Q. Cao, W.P. Cai, Y. Li, F.Q. Sun, L.D. Zhang, *Nanotechnology* 16 (2005) 1734;
(c) Y.H. Leung, A.B. Djurisic, J. Gao, M.H. Xie, Z.F. Wei, S.J. Xu, W.K. Chan, *Chem. Phys. Lett.* 394 (2004) 452;
(d) Y. Chen, D.M. Bagnall, H. Koh, K. Park, K. Hiraga, Z. Zhu, T. Yao, *J. Appl. Phys.* 84 (1998) 3912.
- [13] M.H. Huang, S. Mao, H. Feick, H. Yan, Y. Wu, H. Kind, E. Weber, R. Russo, P. Yang, *Science* 292 (2001) 1897.
- [14] L. Guo, Y.L. Ji, H.B. Xu, P. Simon, Z.Y. Wu, *J. Am. Chem. Soc.* 124 (2002) 14864.
- [15] S.J. Chen, Y.C. Liu, C.L. Shao, R. Mu, Y.M. Lu, J.Y. Zhang, D.Z. Shen, X.W. Fan, *Adv. Mater.* 17 (2005) 586.
- [16] (a) Z.W. Pan, Z.R. Dai, Z.L. Wang, *Science* 291 (2001) 1947;
(b) X.S. Fang, C.H.Y.L.D. Zhang, Y.L.Z.D. Xiao, *Chem. Lett.* 34 (2005) 436.
- [17] (a) Z.L. Wang, X.Y. Kong, Y. Ding, P.X. Gao, W.L. Hughes, R. Yang, Y. Zhang, *Adv. Funct. Mater.* 14 (2004) 943;
(b) G.Z. Shen, J.H. Cho, C.J. Lee, *Chem. Phys. Lett.* 401 (2005) 414.
- [18] J. Zhang, L. Sun, C. Liao, C. Yan, *Chem. Commun. (Cambridge)* 3 (2002) 262.
- [19] (a) J.J. Wu, S.C. Liu, C.T. Wu, K.H. Chen, L.C. Chen, *Appl. Phys. Lett.* 81 (2001) 1312;
(b) J.S. Jeong, J.Y. Lee, J.H. Cho, H.J. Suh, C.J. Lee, *Chem. Mater.* 17 (2005) 2752.
- [20] R.M. Wang, Y.J. Xing, J. Xu, D.P. Yu, *New J. Phys.* 5 (2003) 115.
- [21] J.Q. Hu, Y. Bando, *Appl. Phys. Lett.* 82 (2003) 1401.
- [22] X.W. Sun, S.F. Yu, C.X. Xu, C. Yuen, B.J. Chen, S. Li, *Jpn. J. Appl. Phys. (Part 2)* 42 (2003) L1229.
- [23] Q.C. Li, V. Kumar, Y. Li, H.T. Zhang, T.J. Marks, R.P.H. Chang, *Chem. Mater.* 17 (2005) 1001.
- [24] X.H. Zhang, S.Y. Xie, Z.Y. Jiang, X. Zhang, Z.Q. Tian, Z.X. Xie, R.B. Huang, L.S. Zheng, *J. Phys. Chem. B* 107 (2003) 10114.
- [25] J. Zhang, L.D. Sun, H.Y. Pan, C.S. Liao, C.H. Yan, *New J. Chem.* 26 (2002) 33.
- [26] (a) H. Zhang, D. Yang, X. Ma, Y. Ji, J. Xu, D. Que, *Nanotechnology* 15 (2004) 622;
(b) H. Zhang, D. Yang, Y. Ji, X. Ma, J. Xu, D. Que, *J. Phys. Chem. B* 108 (2004) 3955.
- [27] (a) Z. Li, Y. Xiong, Y. Xie, *Inorg. Chem.* 42 (2003) 8105;
(b) J.P. Liu, X.T. Huang, J.X. Duan, H.H. Ai, P.H. Tu, *Mater. Lett.* 59 (2005) 3710.
- [28] Z.H. Kang, E.B. Wang, M. Jiang, S.Y. Lian, Y.G. Li, C.W. Hu, *Eur. J. Inorg. Chem.* 370 (2003).